

Physical Modelling of Flow and Head along with Dead-end and Looped Manifolds

Abdullah Amer¹, Thamer Ahmad Mohammad^{1*}, Wissam Hameed Alawee² and Nadhir Al-Ansari³

¹Department of Water Resources Engineering, College of Engineering, University of Baghdad, 10070 Jadriyah, Baghdad, Iraq

²Department of Systems and Control Engineering, University of Technology, 10055 Industrial Street, Baghdad, Iraq

³Department of Civil, Environmental and Natural Resources Engineering, Lulea University of Technology, Lulea 971 87, Lulea, Sweden

ABSTRACT

In this study, physical models were designed and fabricated to investigate the hydraulic behaviour of dead-end and looped PVC manifolds. The physical models consisted of a water supply tank with overflow, PVC manifolds, steel supports, collection tank, pump, pressure sensors and valves to allow flow control. Throughout the study, the water level in the supply tank was kept constant. The hydraulic behaviour of dead-end manifolds was investigated using different spacing, S between outlets ($S=3\text{m}$, $S=2.5\text{m}$, $S=2\text{m}$, $S=1.5\text{m}$, and $S=0.75\text{m}$). The hydraulic behaviour of looped manifolds was investigated using a single outlet spacing of 1.5m . The comparison between the hydraulic behaviour of looped and dead-end manifolds was carried out using the data of the 1.5m outlet spacing. The value of uniformity, U for dead-end and looped manifolds was 82% and 92% , respectively. The value of friction ratio, f_n/f_1 , was found to be 33 and 0.18 for dead-end and looped manifolds, respectively. The experimental data of this study were used to validate selected formulae for

estimation of the friction correction factor (G Factor). The results showed that the equation proposed by Alazba et al. (2012) yielded the most satisfactory estimation. The performance of the selected formulae was tested using two statistical indices.

ARTICLE INFO

Article history:

Received: 05 December 2020

Accepted: 21 May 2021

Published: 22 September 2021

DOI: <https://doi.org/10.47836/pjst.29.4.04>

E-mail addresses:

a.rihan1910m@coeng.uobaghdad.edu.iq (Abdullah Amir)

tthamer@gmail.com (Thamer Ahmad Mohammad)

wissam_772005@yahoo.com (Wissam Hameed Alawee)

nadhir.alansari@ltu.se (Nadhir Al-Ansari)

* Corresponding author

Keywords: Dead-end manifold, friction correction factor, hydraulic behaviour, looped manifolds, statistical indices

INTRODUCTION

A manifold can be defined as a pipe with lateral openings (multiple outlets) distributed along its centreline with a known length, diameter and inlet pressure. Depending on the flow mechanism in the manifold, the manifold can be categorised as dividing, combining, parallel or a reverse flow type (Gandhi et al., 2012). Manifolds are used in various engineering applications. For example, in civil engineering, manifolds are widely used in water supply and wastewater projects. In contrast, mechanical engineering used manifolds for fuel distribution. In chemical engineering, manifolds are used for the distribution of chemicals to industrial units. In the design of manifolds, usually, the flow from outlets, coefficient of friction and the friction correction factor are assumed to be constant. Several experimental and mathematical studies have been carried out to investigate manifold hydraulics. The studies focused on the uniformity, hydraulics of sloped manifold and friction correction factor.

The uniformity was studied by Howland (1935), Mokhtari et al. (1997), Koh et al. (2003), Mostafa (2004), Provenzano and Pumo (2004), Maharudrayya et al. (2005), Hassan et al. (2014a), Hassan et al. (2014b), Hassan et al. (2014c), Tong et al. (2009), Sadeghi and Peter (2011), Hassan et al. (2015) and Alawee et al. (2016 & 2019). The impact of the coefficient of friction, friction head loss, manifold dimensions, and manifold slope on the flow from manifold outlets was studied by Mohammed et al. (2003), Keller and Bliesner (1990), Vallesquino and Luque-Escamilla (2002), Yildirim (2007), Alawee et al. (2020) and Sadeghi and Peters (2011). The friction correction factor is commonly used to calculate the total friction head loss along a manifold. Table 1 shows the formulae used to calculate the friction correction factor. Most of the studies referenced above were conducted on dead-end manifolds. Hence, there is a lack of studies on the hydraulics of looped manifolds. The effect of looping in a manifold is expected to reduce friction head losses and improve water flow uniformity. Therefore, an experimental study that compares the hydraulic performances of two different manifold designs is essential. This study will focus on the design, fabrication, installation, and operation of dead-end and looped manifolds. The data collected from the manifolds will be used to evaluate the uniformity, friction head losses, and validation of selected formulae for friction correction factors (Table 1).

MATERIALS AND METHODS

Description of the Experimental Setup

The physical model used in this study was fabricated in the University of Technology, Baghdad, Iraq workshop. The model was composed of a steel water supply tank (total volume = 3.9m³) with dimensions of 1.25m × 1.25m × 2.5m (length × width × height), and it was connected to a horizontal PVC pipe with a diameter of 25.4mm and a length of 18m. The 25.4mm diameter PVC pipe was levelled and laid horizontally on steel supports

Table 1
Selected formulae for friction correction factor

Author	Formula	Equation	Details
Christiansen (1942)	$G = \frac{1^m + 2^m + \dots + N^m}{N^{m+1}}$	1	N=number of outlets, m = power of velocity in friction head
Anwar (1999)	$G = \frac{1}{N^{m+1} + r^m} \sum_{k=1}^N (k + Nr)^m$	2	loss formula, r = outflow discharge to the total discharge, k = integer representing pipe section under consideration,
Oron and Walker (1981)	$G = 0.6387N^{-1.8916} + 0.35929$	3	
Valiantzas (2002)	$G = \frac{1}{m+1} \left[\left(1 + \frac{1}{2N}\right)^{m-1} - \left(\frac{1}{2N}\right)^{m+1} \right]$	4	
Mostafa (2004)	$G = \frac{N^2 + (N-1)^2 + (N-2)^2 + \dots + (N-(N-1))^2}{N^3}$	5	
Mohammed et al. (2003)	$G = \frac{\sum_{i=1}^{N-1} (N-1)^m}{N^{m+1}}$	6	$e=2.71$ and G = friction correction factor
Alazba et al. (2012)	$G = \frac{1 + \frac{1}{m}}{e\pi}$	7	

distributed at intervals of 1.15m. In order to maintain a constant water level of 2.76m in the supply tank, a 100mm diameter overflow PVC pipe was connected at the top of the tank. When the water level in the tank exceeded the level of 2.76m, the surplus water was discharged by gravity through the overflow pipe to a ground tank. Next, to keep the water level in the tank constant, recirculation of water was carried out by pumping the water stored in the ground tank to the supply tank via a 25.4mm diameter supply pipe. In practice, manifolds are subjected to a fixed head. For this reason, a constant head of 2.76m was maintained in the supply tank throughout this study.

In addition, heads greater than 2.76m would have been difficult to achieve due to a limited water supply capacity in the laboratory. Piezometers located at the pipe inlet and outlet were used to determine the head difference/friction head loss along the pipe. For five different velocities, data on friction head loss along the pipe without outlets were measured. The relationship between the friction head loss and the velocity was plotted on a log-log paper. Dead-end manifolds with 6mm diameter outlets distributed longitudinally along their centrelines were used in this study. In order to measure the head/pressure at each outlet, 6mm diameter holes were drilled on the opposite side of the outlets. Each opening was connected to a sensor that feeds into a data logger. The data logger was connected to a computer to obtain each outlet's instantaneous head/pressure readings. In addition, data on head and discharge along the length of dead-end manifolds with different outlet spacing (0.75m, 1.5m, 2.0m, 2.5m and 3.0m) were measured. Figure 1 shows a general three-

dimensional schematic drawing of the dead-end manifold used in this study. Triangular looped manifold, rectangular looped manifold and dead-end (straight) manifold were hydraulically assessed to study the impact of different manifold designs on flow uniformity and friction head losses.

The assessed manifolds had the same diameter (25.4mm), length (18m) and spacing between outlets (1.5m). In comparison, the water level in the supply tank was kept constant at 2.76m. Figures 2 and 3 show the configuration of triangular and rectangular looped manifolds. At the same time, Table 2 illustrates a sample of the sensors digital pressure reading. Each sensor can read a pressure between 0 to 26.85 kN/m² (30 psi)

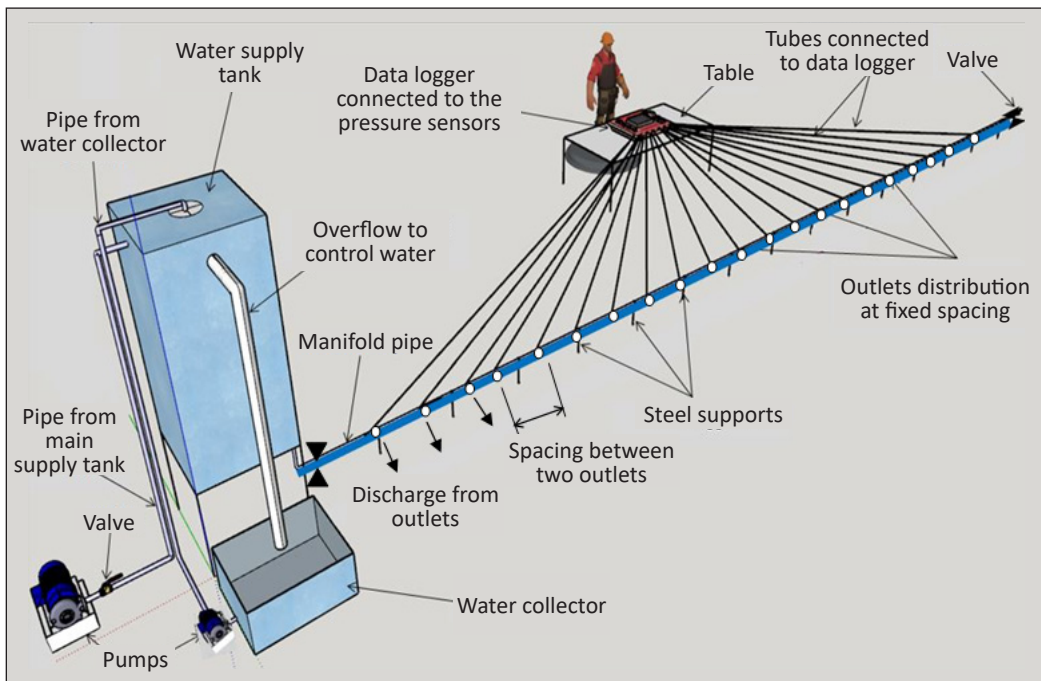


Figure 1. Three-dimensional schematic drawing for the dead-end manifold

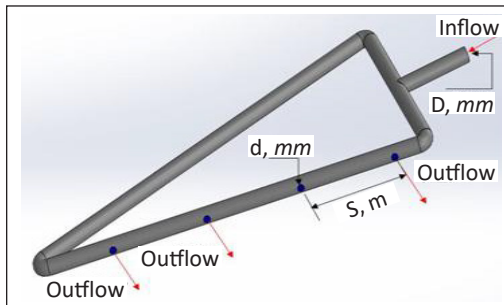


Figure 2. The triangular looped manifold
 Note. D is outlet diameter; d is manifold diameter; S is spacing between outlets

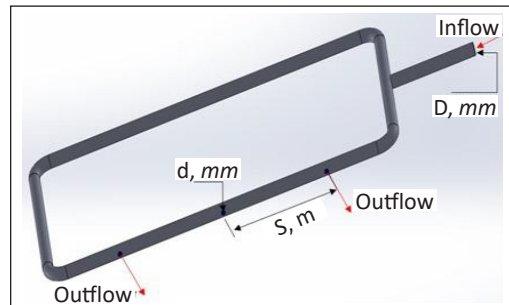


Figure 3. The rectangular looped manifold
 Note. D is outlet diameter; d is manifold diameter; S is spacing between outlets

Table 2
A sample of the sensors reading displayed on the computer screen

Date	Time	Sensors					
		1	2	3	4	5	6
22/10/2019	12:02:06 PM	0	0	0	0	0	0
22/10/2019	12:02:13 PM	3.57	3.61	3.46	3.68	3.68	3.57
22/10/2019	12:02:21 PM	3.64	3.71	3.46	3.46	3.68	3.53
22/10/2019	12:02:28 PM	3.68	3.68	3.57	3.57	3.64	3.5
22/10/2019	12:02:35 PM	3.64	3.64	3.46	3.46	3.68	3.53
22/10/2019	12:02:43 PM	3.68	3.68	3.82	3.57	3.57	3.5
22/10/2019	12:02:50 PM	3.64	3.64	3.46	3.46	3.68	3.53
22/10/2019	12:02:57 PM	3.64	3.71	3.46	3.46	3.46	3.46
22/10/2019	12:03:05 PM	3.5	3.5	3.68	3.68	3.57	3.57
22/10/2019	12:03:12 PM	3.57	3.61	3.46	3.68	3.57	3.46
22/10/2019	12:03:19 PM	3.68	3.86	3.64	3.57	3.46	3.46
22/10/2019	12:03:27 PM	3.68	3.82	3.57	3.57	3.57	3.46
22/10/2019	12:03:34 PM	3.64	3.86	3.57	3.46	3.46	3.46
22/10/2019	12:03:41 PM	3.64	3.71	3.46	3.46	3.46	3.46
22/10/2019	12:03:49 PM	3.46	3.68	3.68	3.57	3.64	3.57
22/10/2019	12:03:56 PM	3.68	3.68	3.68	3.57	3.64	3.5
22/10/2019	12:04:03 PM	3.64	3.86	3.57	3.46	3.46	3.46
22/10/2019	12:04:11 PM	3.68	3.68	3.57	3.57	3.57	3.5
22/10/2019	12:04:18 PM	3.64	3.64	3.46	3.46	3.68	3.53
22/10/2019	12:04:25 PM	3.68	3.86	3.64	3.57	3.46	3.46
22/10/2019	12:04:33 PM	3.64	3.61	3.46	3.46	3.68	3.57
22/10/2019	12:04:47 PM	3.68	3.79	3.5	3.46	3.5	3.68
22/10/2019	12:04:55 PM	3.82	3.86	3.64	3.5	3.46	3.46

with an accuracy of 3%. A piezometer was used to measure the pressure at each outlet to countercheck the readings obtained from the sensors. Hence, the head at the manifold outlet h_i is measured by a sensor and a piezometer. Figure 4 show samples of data collected by the sensors and piezometers along the length of a dead-end manifold. In contrast, Figure 5 shows the calibration curve for the sensors. Table 3 shows the experimental design of the study.

The Laboratory Measurements

The inlet valve controlled the flow from the tank to the manifolds (either dead-end or looped). The discharge from each manifold outlet, q_i , was measured using a container of known volume and a stopwatch. A digital thermometer measured the water temperature. The water temperature throughout this study ranged between 18 to 20°C. The temperature

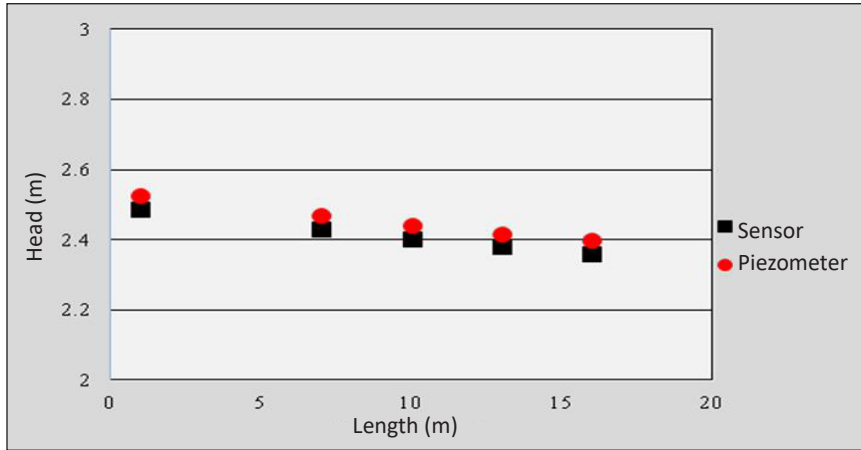


Figure 4. Sensors and piezometers readings for dead-end manifold with spacing, S of 3m

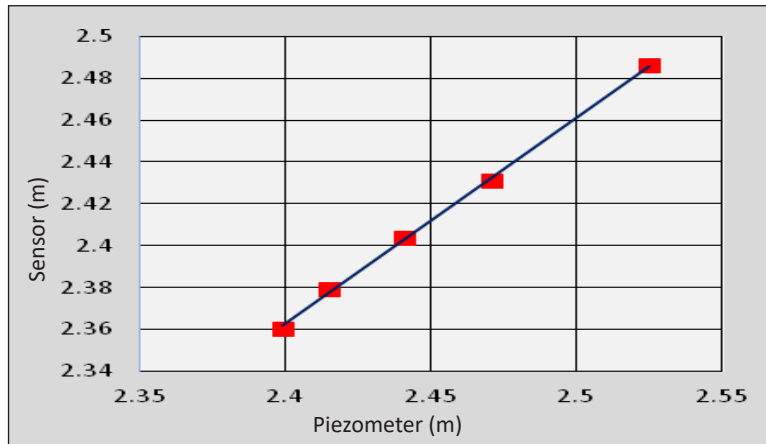


Figure 5. Sensor readings plotted against the piezometer readings for the dead-end manifold with spacing, S of 3m

Table 3
The experimental design

Model type	Diameter	Length	Spacing	Comments
Dead end manifold	25.4 mm	18 m	0.75 m	All manifolds and the normal pipe have the same material and subjected to same pressure at upstream
Dead end manifold	25.4 mm	18 m	0.75 m	
Dead end manifold	25.4 mm	18 m	1.5 m	
Dead end manifold	25.4 mm	18 m	2.0 m	
Dead end manifold	25.4 mm	18 m	2.5 m	
Dead end manifold	25.4 mm	18 m	3.0 m	
Looped triangular manifold	25.4 mm	18 m	1.5 m	
Looped rectangular manifold	25.4 mm	18 m	1.5 m	
Normal pipe (without outlets)	25.4 mm	18 m	1.5 m	

was used to determine the kinematic viscosity of the water. The kinematic viscosity is helpful in the calculation of the Reynolds number at different manifold segments. The difference in head between two successive outlets determines the friction head loss along the manifold segment. For similar flow conditions (discharge and inlet head) and geometry (length and diameter), friction head loss data on dead-end manifolds, looped manifolds and the pipe without outlets were used to calculate the G factors for the dead-end and looped manifolds. In addition, the data was used to validate selected formulae for the G factor.

RESULTS AND DISCUSSION

This study used high precision methods to measure the head and discharge along looped and dead-end manifolds. At each outlet, the discharge was recorded by taking an average of three measurements. At the same time, the head was taken by averaging approximately 30 readings. In addition, the Darcy Weisbach formula was used to calculate the coefficient of friction at different manifold segments. Although the Hazen Williams formula is widely used in the hydraulic design of manifolds (water-supply networks, sprinkler irrigation systems, and drip irrigation systems), its accuracy is affected by the fact that the resistance coefficient is assumed to be a constant value in the calculation of friction head loss in manifolds. Based on the manifold material, the Hazen Williams resistance coefficient is usually provided by the manufacturer. Whereas, if the Darcy Weisbach formula is used for the hydraulic design of manifolds, the value of the coefficient of friction is determined by calculating the Reynolds number and the relative roughness of the manifold. Discharge in manifolds usually decreases towards the dead-end. Hence, the Reynolds number also decreases, which leads to a changing coefficient of friction along the manifold. The values of Reynolds number at different segments of a manifold can be determined if the diameter, velocity, and kinematic viscosity of water at the segments are known.

The size of the PVC manifold used in this study was chosen to be 25.4mm diameter because most drip irrigation systems are designed with PVC manifolds of 25.4mm diameter. So, present study results will improve the hydraulic design of manifolds, particularly those used in drip irrigation systems.

Variation of Discharge and Head along the Dead-end Manifold

Figure 6 show the variations in the head, coefficient of friction and discharge along a dead-end manifold. Due to friction head loss, the head along the manifold is decreasing towards the dead-end. Hence, the discharge is decreasing towards the dead end, as shown in Figure 6. It is confirmed the fact that a discharge from a manifold's outlet, q_i is a function of the head at the outlet, h_i . The spacing between outlets, S is one of the main variables affecting the friction head loss and the variation in discharge along the manifold. In this study, for spacing between outlets, $S = 3$ m, a minimum difference of 5% was obtained between the

discharge of the first and last outlet of the dead-end manifold. In comparison, for $S= 0.75$ m, the maximum difference was 18%. In this study, the uniformity of the flow along a manifold, U , is defined as the ratio of the discharge at the last manifold outlet, q_n , to that at the first outlet, q_1 . It can be expressed as Equation 8.

$$U = \frac{q_n}{q_1} \tag{8}$$

For the ideal case, U 's value is equal to 1, which indicates that the discharge from all manifold outlets is equal. However, in most cases, the value of U is not equal to 1. Therefore, the data on head and discharge at each manifold outlet were collected for various outlet spacing ($S= 3$ m, $S=2.5$ m, $S=2$ m, $S=1.5$ m and $S=0.75$ m). For a maximum spacing of 3m and a minimum spacing of 0.75m, the uniformities were calculated and found to be approximately 95% and 82%, respectively.

The head difference between two successive outlets yielded the friction head loss along the manifold segment between these outlets. In contrast, the head difference between the first and last outlets determines the total friction head loss along the whole manifold. Figures 7, 8 and 9 show the variation of the head, head loss and discharge along with dead-end manifolds with various outlet spacing. For example, for $S= 3$ m and $S=0.75$ m, the total friction head loss along with dead-end manifolds was 0.13m and 0.49m, respectively.

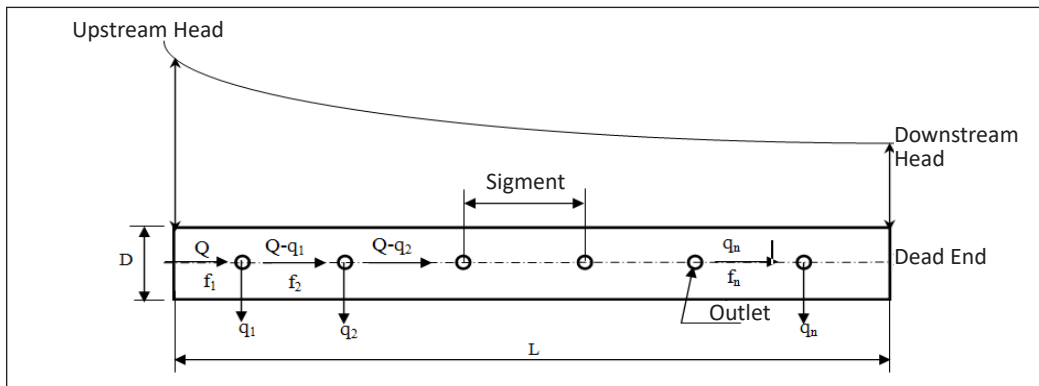


Figure 6. Variation of the head, coefficient of friction in the manifold segment, f_i and discharge from the outlet, q_i along with dead-end manifold (with diameter, d and length, L)

Variation of Discharge and Head along the Looped Manifolds

The distributions of head and discharge along looped manifolds were compared with those of dead-end manifolds. The looped rectangular and the triangular manifolds were symmetrical in geometry, as shown in Figures 2 and 3.

The distribution of head, total head loss and discharge along looped rectangular and triangular manifolds are shown in Figures 10, 11 and 12. The total friction head losses along

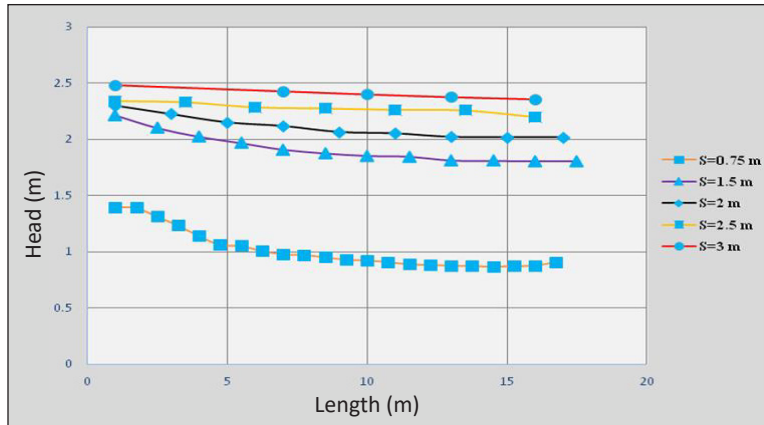


Figure 7. Variation of the head along the dead-end manifolds
 Note. S is the spacing between lines

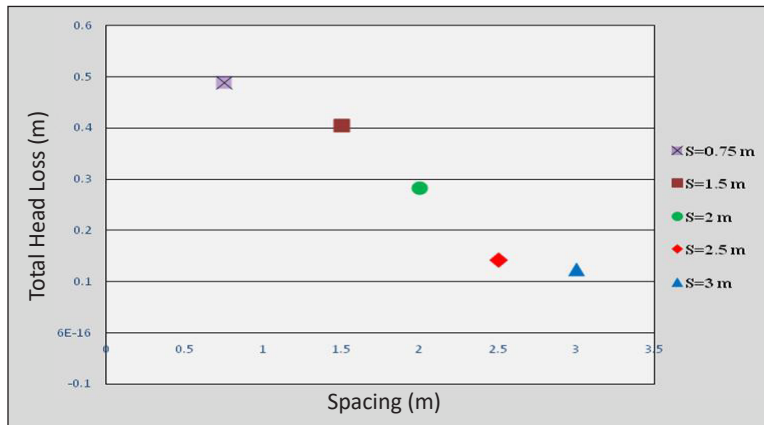


Figure 8. The impact of spacing between outlets on the friction head loss in the dead-end manifold
 Note. S is the spacing between lines

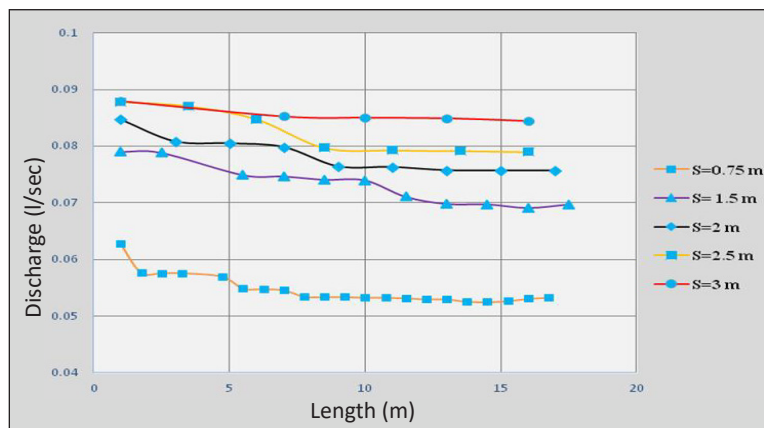


Figure 9. Variation of discharge along with the dead-end manifold
 Note. S is the spacing between lines

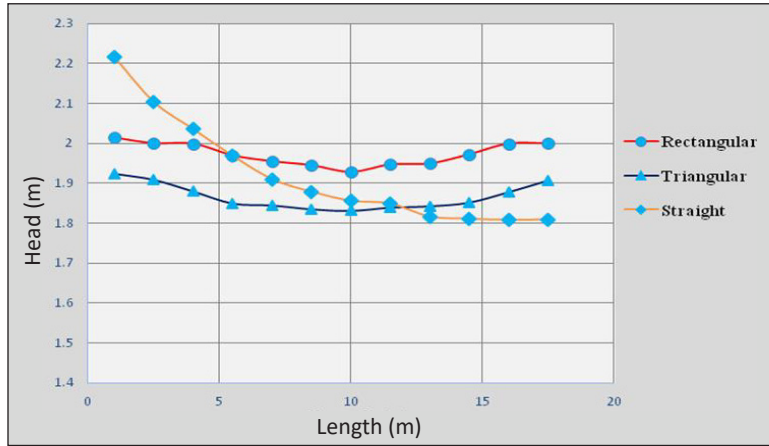


Figure 10. Variation of head along with looped manifolds

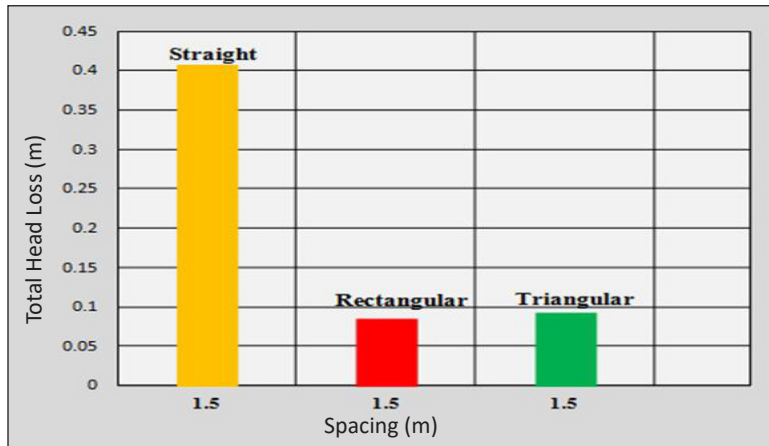


Figure 11. The total head loss in looped manifolds

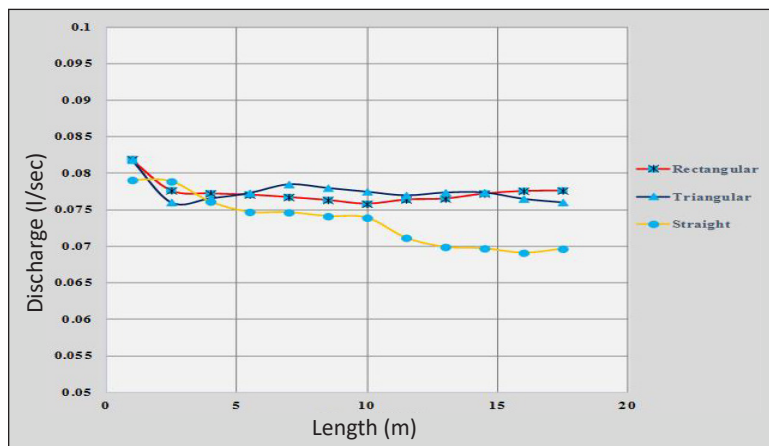


Figure 12. Variation of discharge along with looped manifolds

the triangular and rectangular looped manifolds were 0.071m and 0.092m, respectively. In comparison, the total friction head loss along the dead-end manifold with an outlet spacing of 1.5m, exact dimensions and flow conditions as the triangular and rectangular looped manifolds was found to be 0.41m only. Based on the above findings, the friction head loss in the dead-end manifold was greater than that in the looped manifold by almost 500%. In looped manifolds, the total discharge was divided between two branches of equal lengths of an identical number of outlets. This arrangement leads to reduced friction head losses and hence improved uniformity in the looped manifold. Figures 13 and 14 show the uniformity for dead-end and looped manifolds (rectangular and triangular).

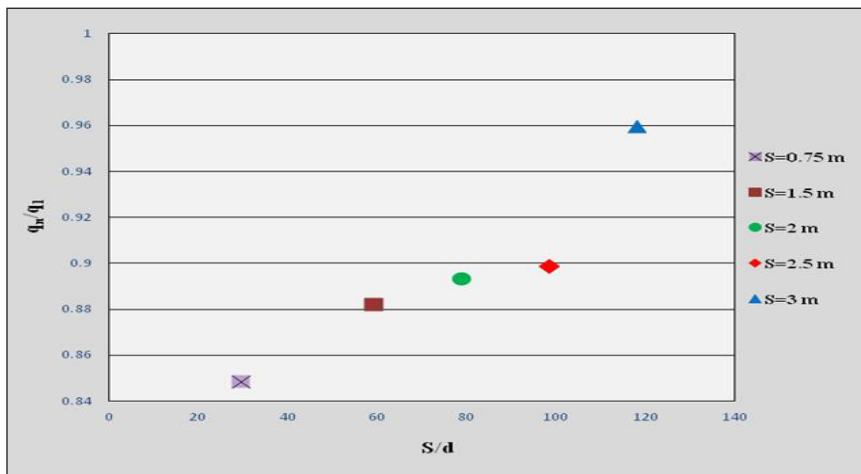


Figure 13. Variation of the uniformity coefficient, q_n/q_1 with spacing ratio, S/d for the dead-end manifold
 Note. S is the spacing in between outlets; d is the manifold diameter

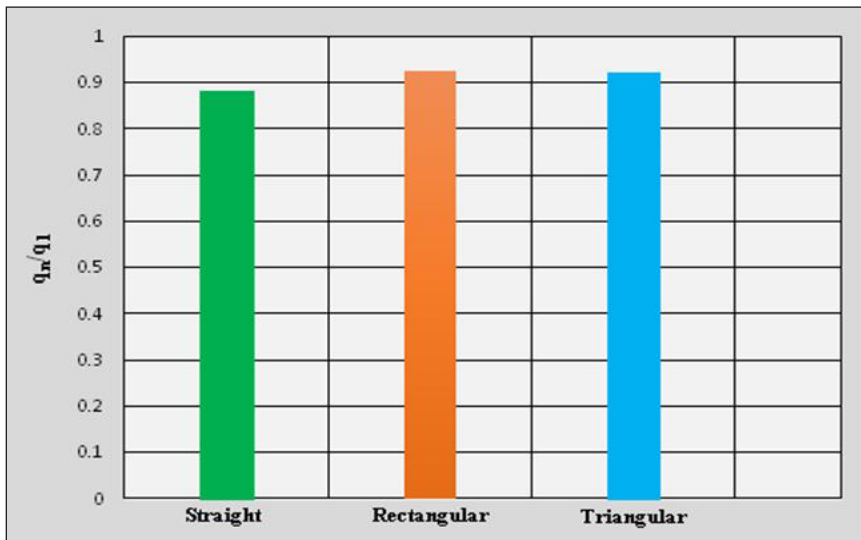


Figure 14. The uniformity coefficient, q_n/q_1 for dead-end (straight), rectangular, and triangular manifold types

The uniformities for the dead-end manifold, looped rectangular manifold and looped triangular manifold were calculated and found to be 82.8%, 91.7% and 92%, respectively. In looped manifolds, there was a gain in the head, which improved the uniformity value. The impact of different ranges of outlet spacing on head loss and uniformity was studied using a dead-end manifold. However, only one range of spacing between outlets (1.5m) was used to study the impact of looping on friction head loss and uniformity. The main objective of the comparison is to demonstrate the effect of looping in reducing the friction head loss and improving the uniformity along a manifold. Many previous studies assumed a constant coefficient of friction, f , while calculating the friction head loss in a manifold (Mohammed et al., 2003). In this study, the data collected from measurements of head and discharge along the manifold were used to calculate the values of coefficient of friction for different manifold segments by applying the Darcy Weisbach Equation 9 described below:

$$f_i = \frac{(h_f)_i d^5 g \pi^2}{8lQ_i^2} \tag{9}$$

where, f_i is coefficient of friction in a manifold segment i , $(h_f)_i$ is the friction head loss along with a manifold segment i , d is manifold diameter, g is the acceleration due to gravity, l is the segment length, Q_i is the discharge in a manifold segment, l and π is constant equal to 3.14.

The coefficient of friction varied widely along the dead-end and looped manifolds, the coefficient of friction in the first manifold segment, f_1 and that in the last segment, f_n can be used to illustrate the variations in the coefficient of friction along with the studied manifolds, the friction ratio, f_n/f_1 was calculated for the studied manifolds. Figures 15 and 16 show the relationship between the friction ratio, f_n/f_1 and the ratio S/d (outlet spacing, S /manifold

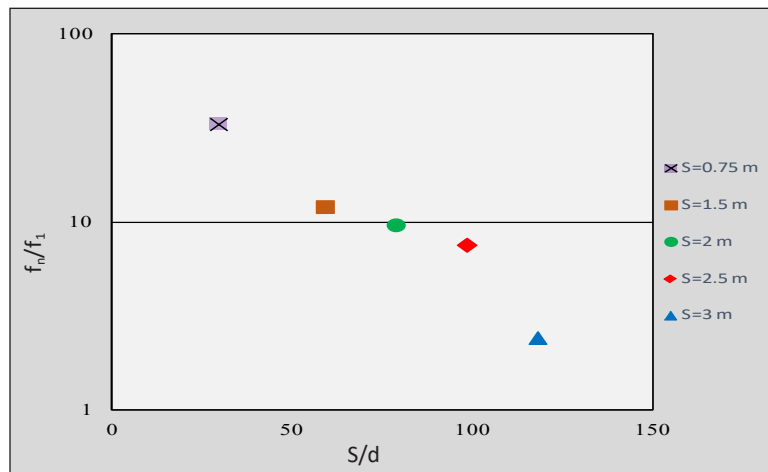


Figure 15. Variation of friction ratio, f_n/f_1 with spacing ratio, S/d in the dead-end manifolds
 Note. S is the spacing between outlets; d is the manifold diameter; f_1 is coefficient friction in the first manifold segment; f_n is the coefficient of friction in the first manifold

diameter, d). For dead-end manifold with a minimum spacing (S=0.75m), the friction ratio was maximum ($f_n/f_1=33$), while for maximum spacing (S=3m), the ratio was minimum ($f_n/f_1=0.18$). For an outlet spacing of 1.5m, the values of f_n/f_1 for rectangular and triangular looped manifolds were found to be 0.134 and 0.028, respectively.

In this study, the Reynolds number was calculated using the following Equation 10:

$$(Re)_i = \frac{4Q_i}{\pi d} \quad (10)$$



Figure 16. The friction ratio, f_n/f_1 for dead-end, rectangular, and triangular manifolds

where, the $(Re)_i$ is the Reynolds number, Q_i is the discharge in a manifold segment i , ν is the kinematic viscosity, d is the manifold diameter and π is constant equal to 3.14.

In this study, the relative roughness of the PVC manifolds was kept constant since single diameter manifolds ($d=25.4\text{mm}$) were used. Figure 17 show the calculated coefficient of frictions and Reynold numbers at various manifold segments.

Under different flow conditions of the present study, the values of Reynolds number ranged from 4000 to 60640, which indicates transitional and turbulent flow. A fitted curve that represents smooth pipe flow behaviour was set through the data. The relationship presented in Figure 17 confirms that the coefficient of friction for a smooth pipe is a

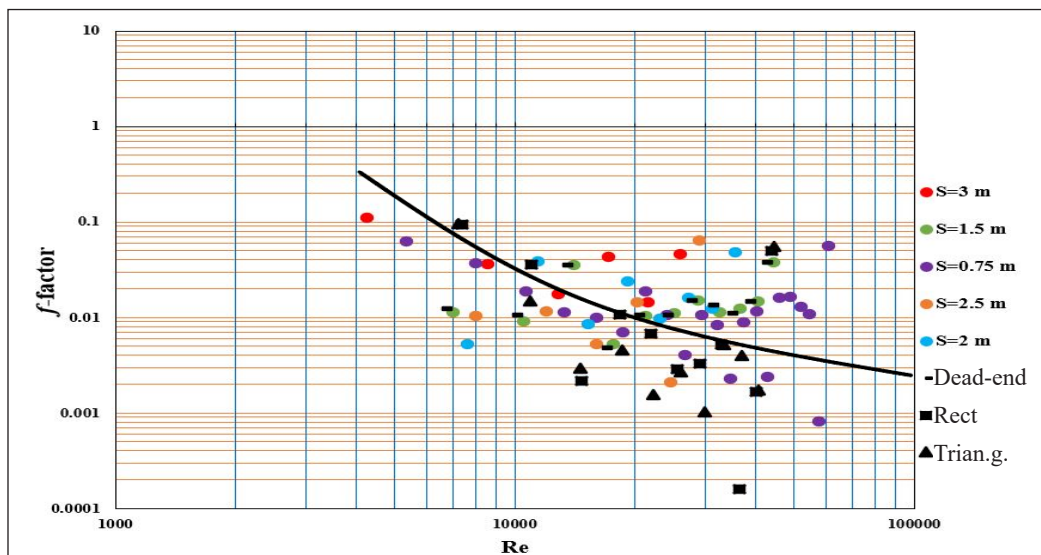


Figure 17. Moody diagram for the studied manifolds (relationship between coefficient of friction, f and Reynolds number, Re)

function of the Reynolds number only. It agree with the relationship given by Blasius for a smooth pipe (Streeter et al., 1998).

Friction Correction Factor for Dead-end and Looped Manifolds

The ratio between the total friction head loss in a manifold to that in a standard pipe having the same material, length, diameter and flow rate but without outlets is called friction correction factor. Researchers termed it the G factor, and it is calculated using Equation 11.

$$G_{\text{factor}} = (h_f)_m / (h_f)_p \quad (11)$$

where $(h_f)_m$ is the total friction head loss in the manifold and $(h_f)_p$ is the total friction head loss in the pipe without outlets.

The G factor can be used to simplify the calculation of friction head losses along a manifold. The present study used experimental data on friction head losses in standard PVC pipe (without outlets), dead-end manifolds and looped manifolds to determine the friction correction factor (G factor). Figure 18 shows the relationship on a log-log plot between friction head loss $(h_f)_p$ and the velocity, v along a PVC pipe without outlets.

The below relationship was obtained from five different discharge measurements taken during the experimental works (Equation 12).

$$(h_f)_p = 0.24 v^2 \quad (12)$$

The G factor for the dead-end manifold was calculated for different spacing, S between outlets ($S=3\text{m}$, $S=2.5\text{m}$, $S=2\text{m}$, $S=1.5\text{m}$ and $S=0.75\text{m}$), while for looped manifolds, only

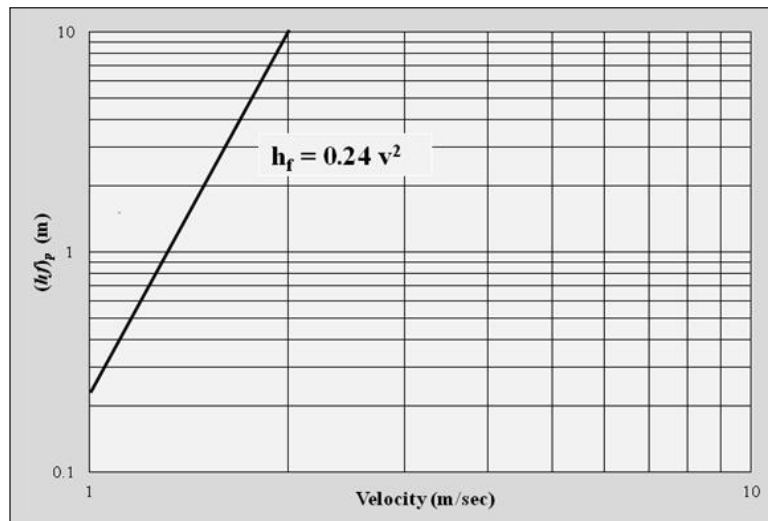


Figure 18. Relationship between the velocity, v and friction head loss for the PVC pipe without outlets $(h_f)_p$

one spacing was studied ($S=1.5\text{m}$). Table 4 and Figures 19 and 20 show the values of the G factor for the tested manifolds. The values of the G factor for the dead-end manifolds were significantly higher than those for looped manifolds.

The maximum value of the G factor in this study was found to be 0.608. It was obtained from friction head loss data of the dead-end manifold, while the minimum value was 0.112, and it was obtained from friction head loss data of the triangular looped manifold.

The values of the G factor in dead-end and lopped manifolds varied due to variation in friction head losses. The experimental data of the present study was used to validate selected formulae for estimation of the friction correction factor (G factor) for manifolds. For the

Table 4
Values of G factor for the studied manifolds

Manifold	L m	S m	N	$(h_f)_m$ m	$(h_f)_p$ m	G factor (from exp. data)
Dead-end	18	0.75	22	0.4888	1.3666	0.3577
Dead-end	18	1.5	12	0.4063	0.7315	0.5554
Dead-end	18	2	9	0.283	0.4655	0.6079
Dead-end	18	2.5	7	0.1436	0.3111	0.4616
Dead-end	18	3	6	0.1253	0.2487	0.5038
Dead-end	18	1.5	12	0.4071	0.7254	0.5612
Rectangular	18	1.5	12	0.0851	0.8049	0.1057
Triangular	18	1.5	12	0.0922	0.8242	0.1119
Dead-end	18	0.75	22	0.4888	1.3666	0.3577

L=manifold length, S=spacing between outlets, N=number of spacing, $(h_f)_m$ = friction head loss in manifold, $(h_f)_p$ = friction head loss in pipe without outlets, G=friction correction factor

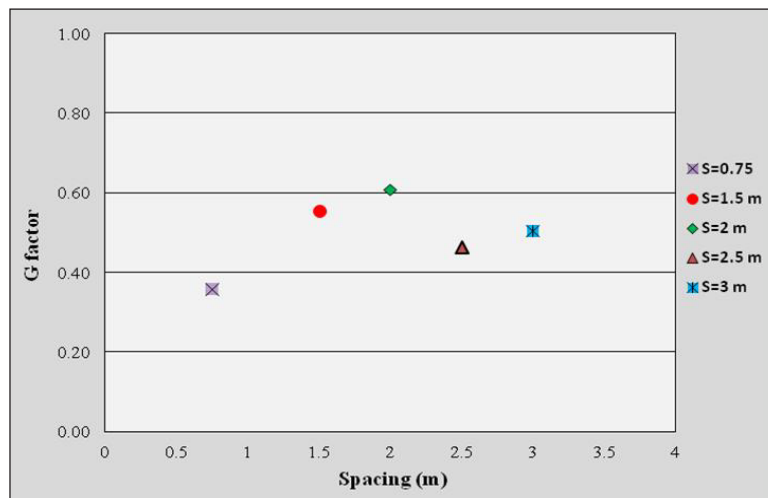


Figure 19. Variation of G factor (friction correction factor) with the outlet spacing, S for the dead-end manifold

dead-end manifolds used in this study, the G factor obtained from the experimental data for different outlet spacing was compared with that calculated using selected formulae, as shown in Table 5.

In this study, the tested formulae for the G factor were the formulae proposed by Christiansen (1942), Albertson et al. (1960), Mostafa (2004), Mohammed et al. (2003), Oron and Walker (1981), Valiantzas (2002), and Alazba et al. (2012). The G factor in

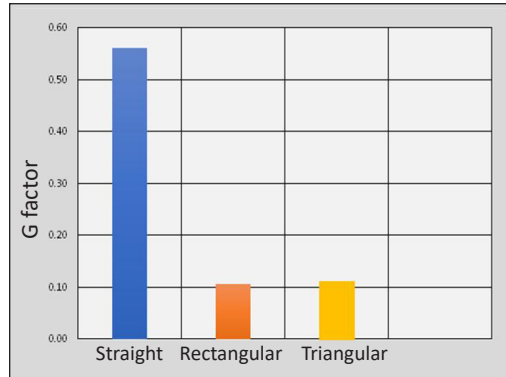


Figure 20. Values of G factor (friction correction factor) for the studied manifolds

Table 5
Values of G factor from the selected formulae and from the experimental data

	N=22	N=12	N=9	N=7	N=6
Experimental G factor	0.3577	0.5554	0.6079	0.4616	0.5038
Christiansen (1942)	0.3564	0.3762	0.3909	0.4082	0.4213
Albertson et al. (1960)	0.3333	0.3333	0.3333	0.3333	0.3333
Oron and Walker (1981)	0.3611	0.3651	0.3693	0.3754	0.3808
Valiantzas (2002)	0.3566	0.3767	0.392	0.4099	0.4236
Mostafa (2004)	0.3564	0.3762	0.3909	0.4082	0.4213
Mohammed et al. (2003)	0.311	0.2928	0.2798	0.2653	0.2546
Alazba et al. (2012)	0.5531	0.5732	0.5879	0.6047	0.6173

these formulae was either a function of the number of outlets in a manifold, N, only or a function of both number of outlets, N and the velocity exponent, m. Thus, the general relationship between the friction head loss, h_f and velocity, v in a pipe can be expressed in the following parabolic form (Equation 13):

$$h_f = Cv^m \tag{13}$$

where C is a constant number, and m is an exponent equal to 2 in Darcy Weisbach equation and 1.85 in Hazen Williams equation.

The comparison between Equations 12 and 13 determined that the value of the velocity exponent, m was 2.

Figure 21 show that most of the tested formulae underestimated the value of the G factor. Therefore, to study the impact of the outlets' number, N, on the G factor, the values were plotted as shown in Figure 22. For example, the value of the velocity exponent, m, was taken as 1.85 by Mostafa (2004), Alazba et al. (2012), and Sadeghi and Peters (2011).

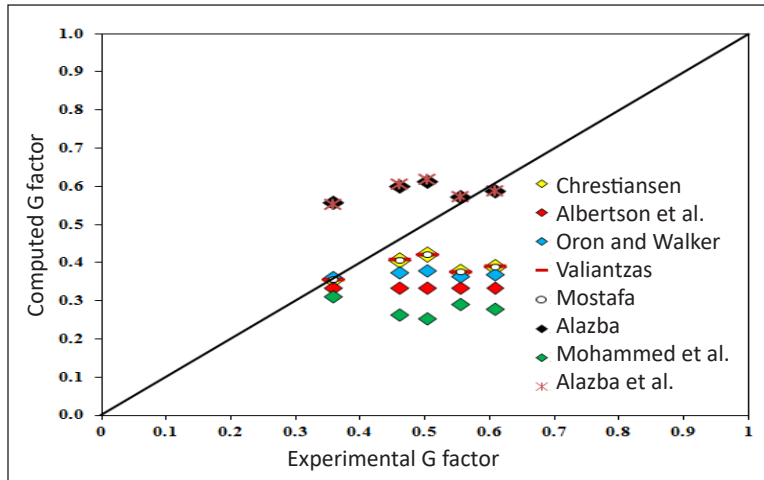


Figure 21. The validation of the selected G factor formulae

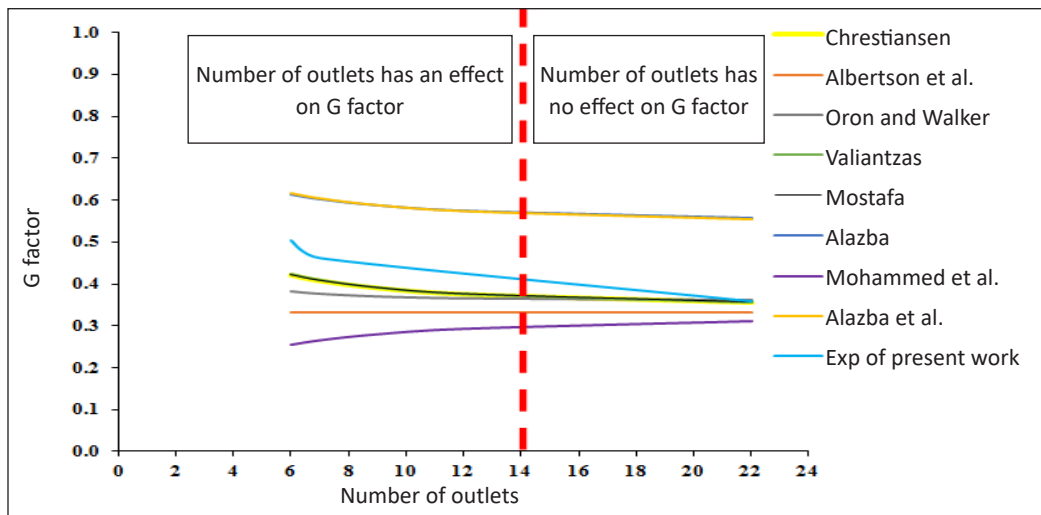


Figure 22. Variation of G factor with the number of manifold outlets

Statistical Tests

The agreement between the values of the experimental G factor and that computed from the application of selected formulae were tested using two statistical indices; the root mean square deviation (RMSD) (Equation 14) and normalised root mean squared deviation (NRMSD) (Equation 15).

$$RMSD = \sqrt{\frac{\sum_{i=1}^n (G_{e,i} - G_{c,i})^2}{n}} \quad (14)$$

$$\text{NRMSD} = \frac{\text{RMSD}}{G_{\max} - G_{\min}} \quad (15)$$

where $G_{e,i}$ represents the value of the experimental G factor, $G_{c,i}$ represents the values of computed G factor obtained from the tested formulae, n = number of experimental data, G_{\max} is the value of the maximum experimental G factor, G_{\min} is the value of the minimum experimental G factor.

In statistics, RMSD is commonly used to compare calculated and measured values and obtain an indication of the accuracy of the model predictions (Legates and McCabe, 1999). A low RMSD or NRMSD indicate an accurate prediction. Table 6 show the values of the selected statistical indices for all the tested formulae. Table 6 shows that the formulae proposed by Alazba et al. (2012) gave the lowest values for RMSD and NRMSD. These values were 0.120, 0.480, respectively. Based on the above results, it can be concluded that the Alazba et al. (2012) formula gave the most accurate estimation for the G factor.

Table 6
The statistical indices for the selected formulae of G factor

Formula for G Factor	RMSD	NRMSD
Christiansen (1942)	0.133	0.533
Albertson et al. (1960)	0.185	0.739
Oron and Walker (1981)	0.152	0.608
Valiantzas (2002)	0.132	0.529
Mostafa (2004)	0.133	0.533
Mohammed et al. (2003)	0.236	0.945
Alazba et al. (2012)	0.120	0.480

From the above discussion, the engineering significance of the present study can be summarised as:

1. The friction head loss and discharge variation along dead-end and looped manifolds were studied using reliable experimental data. The impact of looping of manifolds on uniformity and friction head losses was highlighted.
2. For both dead-end and looped manifolds, the experimental data confirmed that the coefficient of friction varied at various manifold segments. It confirms that using a constant value for the coefficient of friction along a manifold affects the accuracy of the hydraulic design. In addition, it is more suitable to use the Darcy Weisbach formula in the hydraulic design of manifolds as it allows for the use of different coefficient of friction values in the calculation. It is not possible in the Hazen Williams formula since it only assigns one value of the resistance coefficient along the entire manifold.

3. The manifold diameter used in this study was 25.4mm. The size and material of the manifold are widely used in drip irrigation systems around the world. So, the present study results can be used to improve the hydraulic design of drip irrigation systems.
4. The experimental data were used to validate selected formulae for the G factor, and a recommendation on the reliability of these formulae was given based on the statistical tests. Thus, it will assist manifold designers to apply a suitable formula.

CONCLUSION

The physical models of dead-end and looped PVC manifolds were designed and fabricated to test the variation of discharge and head losses along with these manifolds. For manifolds with the same length, diameter and material, the outlets spacing and manifold type (looped or dead-end) are the main factors affecting the friction head losses and uniformity. The study concluded a proportional relationship between spacing ratio, S/d (ratio of the spacing between outlets, S to manifold diameter, d), and the uniformity coefficient (q_n/q_1).

In addition, the experimental data showed that the uniformity increased in looped manifolds. The rectangular and the triangular looped manifolds yielded a uniformity of 92%. At the same time, a dead-end manifold with the same characteristics and flow conditions yielded a uniformity of 82%. The study also concluded that friction head losses were significantly less in looped manifolds than dead-end manifolds. For the same diameter, length, outlet spacing, material and inlet head, the friction head loss in the dead-end manifold was approximately 500% higher than that in the looped manifold because looping reduces the flow length and discharge. Therefore, the variation in the coefficient of friction along the dead-end manifold was significant. Hence, it should be considered in the hydraulic design. The maximum value of friction ratio, f_n/f_1 , was found to be 33. From collected data, the relationship between the Reynolds number and the coefficient of friction was found to be within the smooth region of Moody's diagram (Reynolds number between 4000 and 100000).

It was also found that the primary variable affecting the friction correction factor (G factor) is the spacing between outlets along the manifold (or the number of outlets). The study results show that when the number of outlets in a manifold was 14 or less, the impact was significant on the G factor. Also, the values of the G factor were significantly reduced in looped manifolds (rectangular or triangular). Validation of selected formulae of the G factor revealed that most of them underestimated the values of the G factor. Statistical tests were made to assess the performance of the selected formulae. The formula proposed by Alazba et al. (2012) yielded the most satisfactory estimation among the eight tested formulae. The tested formulae' performance was assessed using two statistical indices, and these indices were RMSD and NRMSD. The values of these indices for the equation of Alazba et al. (2012) were 0.120 and 0.480, respectively.

ACKNOWLEDGEMENT

The authors acknowledged the technical support provided by the Workshops and Training Center at the University of Technology, Baghdad, Iraq.

REFERENCES

- Alawee, W. H., Almolhem, Y. A., Yusuf, B., Mohammad, T. A., & Dhahad, H. A. (2020). Variation of coefficient of friction and friction head losses along a pipe with multiple outlets. *Water*, *12*(844), 1-15. <https://doi.org/10.3390/w12030844>
- Alawee, W. H., Hassan, J. M., & Mohammad, W. S. (2016). Experimental and numerical study on the improvement of uniformity flow in a parallel flow channel. *Engineering and Technology Journal*, *34*(5), 847-856.
- Alawee, W. H., Yusuf, B., Mohammad, T. A., & Dhahad, H. A. (2019). Variation of flow along a multiple outlets pipe with various spacing and inflow water head based on physical model. *Journal of Engineering Science and Technology*, *14*(4), 2399-2409.
- Alazba, A. A., Mattar, M. A., El-Nesr, M. N., & Amin, M. T. (2012). Field assessment of friction head loss and friction correction factor equations. *Journal of Irrigation and Drainage Engineering, ASCE*, *138*(2), 166-176. [https://doi.org/10.1061/\(ASCE\)IR.1943-4774.0000387](https://doi.org/10.1061/(ASCE)IR.1943-4774.0000387)
- Albertson, M. L., Bartion, J. R., & Simons, D. B. (1960). *Fluid Mechanics for Engineers*. Prentice Hall.
- Anwar, A. A. (1999). Factor G for pipeline with equally spaced multiple outlets and outflow. *Journal of Irrigation and Drainage Engineering, ASCE*, *125*(1), 34-38. [https://doi.org/10.1061/\(ASCE\)0733-9437\(1999\)125:1\(34\)](https://doi.org/10.1061/(ASCE)0733-9437(1999)125:1(34))
- Christiansen, J. (1942). *Irrigation by sprinkling*. University of California, Agricultural Experiment Station Bulletin.
- Gandhi, M. S., Ganguli, A. A., Joshi, J. B., & Vijayan, P. K. (2012). CFD simulation for steam distribution in header and tube assemblies. *Chemical Engineering Research and Design*, *90*(4), 487-506. <https://doi.org/10.1016/j.cherd.2011.08.019>
- Hassan, J. M., Mohamed, T. A., Mohammed, W. S., & Alawee, W. H. (2014a). Modeling the uniformity of manifold with various configurations. *Journal of Fluids*, *2014*, Article 325259. <https://doi.org/10.1155/2014/325259>
- Hassan, J. M., Mohammed, W. S., Mohamed, T. A., & Alawee, W. H. (2014b). Review on single-phase fluid flow distribution in manifold. *International Journal of Science and Research*, *3*(1), 325-330.
- Hassan, J. M., Mohammed, W. S., Mohamed, T. A., & Alawee, W. H. (2014c). CFD simulation for manifold with tapered longitudinal section. *International Journal of Emerging Technology and Advanced Engineering*, *4*(2), 28-35.
- Hassan, J. M., Mohamed, T. A., Mohammed, W. S., & Alawee, W. H. (2015). Experimental and numerical study on the improvement of uniformity flow for three-lateral dividing manifold. *International Journal of Engineering and Technology*, *12*(1), 29-37.

- Howland, W. E. (1935). Gain in head at take-offs. *Journal of the New England Water Works Association*, 49(1), Article 14.
- Keller, J., & Bliesner, R. D. (1990). *Sprinkle and trickle irrigation*. Springer Science + Business Media.
- Koh, J. H., Seo, H. K., Lee, C. G., Yoo, Y. S., & Lim, H. C. (2003). Pressure and flow distribution in internal gas manifolds of a fuel-cell stack. *Journal of Power Sources*, 115(1), 54-65. [https://doi.org/10.1016/S0378-7753\(02\)00615-8](https://doi.org/10.1016/S0378-7753(02)00615-8)
- Legates, D. R., & McCabe, J. (1999). Evaluating the use of “goodness-of fit” measures in hydrologic and hydroclimatic model validation. *Water Resources Research*, 35(1), 233-241. <https://doi.org/10.1029/1998WR900018>
- Maharudrayya, S., Jayanti, S., & Deshpande, A. P. (2005). Flow distribution and pressure drop in parallel-channel configurations of planar fuel cells. *Journal of Power Sources*, 144, 94-106. <https://doi.org/10.1016/j.jpowsour.2004.12.018>
- Mohammed, T. A., Noor, M. J. M. M., Halim, A. G., Badronnisa, Y., Soom, M. A. M., & Benzagta, M. A. M. (2003). Experimental study on the friction loss and uniformity of lateral discharge along a manifold. *Journal of Institution of Engineers Malaysia*, 64(2), 20-25.
- Mokhtari, S., Kudriavtsev, V. V., & Danna, M. (1997). Flow uniformity and pressure variation in multi-outlet flow distribution pipes. *Advances in Analytical, Experimental and Computational Technologies in Fluids, Structures, Transients and Natural Hazards*, 355, 113-122.
- Mostafa, E. A. (2004, March 26-28). Correction factor for friction head loss through lateral and manifold. In *Eighth International Water Technology Conference IWTC8* (pp. 735-749). Alexandria, Egypt.
- Oron, G., & Walker, W. (1981). Optimal design and operation of permanent irrigation systems. *Water Resources Research*, 17(1), 11-17. <https://doi.org/10.1029/WR017i001p00011>
- Provenzano, G., & Pumo, D. (2004). Experimental analysis of local pressure losses for microirrigation laterals. *Journal of Irrigation and Drainage Engineering*, 130, 318-324. [https://doi.org/10.1061/\(ASCE\)0733-9437\(2004\)130:4\(318\)](https://doi.org/10.1061/(ASCE)0733-9437(2004)130:4(318))
- Sadeghi, S. H., & Peters, T. (2011). Modified G and G_{avg} correction factors for laterals with multiple outlets and outflow. *Journal of Irrigation and Drainage Engineering, ASCE*, 137(11), 697-704. [https://doi.org/10.1061/\(ASCE\)IR.1943-4774.0000332](https://doi.org/10.1061/(ASCE)IR.1943-4774.0000332)
- Streeter, V. L., Wylie, E. B., & Bedford, K. W. (1998). *Fluid mechanics* (9th Ed.). McGraw-Hill Publishing Company.
- Tong, J. C. K., Sparrow, E. M., & Abraham, J. P. (2009). Geometric strategies for attainment of identical outflows through all of the exit ports of a distribution manifold in a manifold system. *Applied Thermal Engineering*, 29(17-18), 3552-3560. <https://doi.org/10.1016/j.applthermaleng.2009.06.010>
- Valiantzas, J. (2002). Continuous outflow variation along irrigation laterals: Effect of the number of outlets. *Journal of Irrigation and Drainage Engineering, ASCE*, 128, 34-42. [https://doi.org/10.1061/\(ASCE\)0733-9437\(2002\)128:1\(34\)](https://doi.org/10.1061/(ASCE)0733-9437(2002)128:1(34))

- Vallesquino, P., & Luque-Escamilla, P. L. (2002). Equivalent friction factor method for hydraulic calculation in irrigation laterals. *Journal of Irrigation and Drainage Engineering*, 128(5), 278-286. [https://doi.org/10.1061/\(ASCE\)0733-9437\(2002\)128:5\(278\)](https://doi.org/10.1061/(ASCE)0733-9437(2002)128:5(278))
- Yildirim, G. (2007). Analytical relationship for designing multiple outlets pipelines. *Journal of Irrigation and Drainage Engineering, ASCE*, 133(2), 140-154. [https://doi.org/10.1061/\(ASCE\)0733-9437\(2007\)133:2\(140\)](https://doi.org/10.1061/(ASCE)0733-9437(2007)133:2(140))